

## THE MASS DEPENDENCE OF DWARF SATELLITE GALAXY QUENCHING

COLIN T. SLATER AND ERIC F. BELL

Department of Astronomy, University of Michigan, 500 Church St., Ann Arbor, MI 48109; ctslater@umich.edu,ericbell@umich.edu

## ABSTRACT

We combine observations of the Local Group with data from the NASA-Sloan Atlas to show the variation in the quenched fraction of satellite galaxies from low mass dwarf spheroidals and dwarf irregulars to more massive dwarfs similar to the Magellanic clouds. While almost all of the low mass ( $M_\star \lesssim 10^7 M_\odot$ ) dwarfs are quenched, at higher masses the quenched fraction decreases to approximately 40-50%. This change in the quenched fraction is large, and suggests a sudden change in the effectiveness of quenching that correlates with satellite mass. We combine this observation with models of satellite infall and ram pressure stripping to show that the low mass satellites must quench within 1-2 Gyr of pericenter passage to maintain a high quenched fraction, but that many more massive dwarfs must continue to form stars today even though they likely fell in to their host  $> 5$  Gyr ago. We also characterize how the susceptibility of dwarfs to ram pressure must vary as a function of mass if it is to account for the change in quenched fractions. Though neither model predicts the quenching effectiveness *a priori*, this modeling illustrates the physical requirements that the observed quenched fractions place on possible quenching mechanisms.

*Subject headings:* galaxies: dwarf — Local Group — galaxies: evolution

## 1. INTRODUCTION

The shut-off of star formation in galaxies presents one of the most central features in galaxy evolution but the physical mechanisms at work, along with the conditions required for quenching, remain poorly constrained. Many mechanisms have been shown to be capable of shutting off star formation, as the underlying requirement of denying cold gas to the galaxy can be met in numerous ways. Broadly speaking, these mechanisms can heat and remove the gas as in ram pressure stripping (Lin & Faber 1983; Mayer et al. 2006) or supernova-driven outflows (Dekel & Silk 1986; Ferrara & Tolstoy 2000; Sawala et al. 2010), or prevent cooling and accretion of gas onto the galaxy to replenish the gas supply (Efstathiou 1992; Gnedin 2000; Dijkstra et al. 2004). In general it can be easily illustrated that each of these routes for quenching star formation can plausibly accomplish the task, but it has been difficult to distinguish which of these mechanisms dominate the quenching process, and under which circumstances.

A fruitful method to help understand the various quenching mechanisms has been to distinguish between a quenching process that occurs in galaxies which are satellites of a larger host galaxy and that which occurs in central galaxies which are the most massive galaxy in their halo (Weinmann et al. 2006; van den Bosch et al. 2008; Tinker & Wetzel 2010). This is motivated both by the long-standing observation that galaxies in dense environments are preferentially quenched compared to those in the field (Dressler 1980; Postman & Geller 1984; Balogh et al. 2004), and by the physical differences between mechanisms which could quench satellite and central galaxies (e.g., an isolated galaxy is unlikely to experience ram pressure stripping, or satellites are unlikely to merge with each other). This distinction in mechanisms was readily incorporated into semi-analytic models (Cole et al. 1994) and tuned to accurately reproduce the distribution of satellite galaxy colors (Font et al. 2008;

Weinmann et al. 2010). Further observations have sought to measure the dependence of quenching on both satellite and host halo mass (Wetzel et al. 2013). For dwarf galaxies with stellar masses between  $10^7$  and  $10^9 M_\odot$  the differentiation between satellites and field galaxies is most acute, as quenched field galaxies are exceedingly rare ( $< 0.06\%$ ) in this range (Geha et al. 2012).

The severity of this cut-off in field galaxy quenching provides a strong motivation to understand how satellite galaxies at similar masses respond to possible quenching mechanisms. Our primary objective in this work is to illustrate how the quenched fraction of satellites varies from LMC-mass galaxies (as in Geha et al. 2012) down to the lowest mass dwarfs we observe in the Local Group. One of the principal challenges for this is to achieve a homogeneous selection of galaxies despite the necessarily heterogeneous parent samples required. Extending our sample to galaxies below roughly  $10^8 M_\odot$  in stellar mass requires including satellites of the Local Group, which cannot be seen elsewhere in wide-area surveys like SDSS. Conversely, galaxies above this mass are infrequent in the Local Group and a larger survey is required to obtain meaningful statistics. As a result of these challenges, covering such large ranges in galaxy mass requires combining heterogeneous samples of the Local Group dwarfs with larger scale samples like SDSS. This is the strategy we adopt in this work, which will enable us to illustrate how the quenching behavior of galaxies changes over five orders of magnitude in mass. From these measurements, we use N-body simulations to translate the observed quenched fractions into physical constraints on possible mechanisms, with the intention of providing guidance to future detailed simulations of the quenching mechanisms themselves.

In this work we will detail the observed datasets, including the various corrections for selection effects, in Section 2, and we describe the resulting quenching fraction behavior in Section 3. This result will then be interpreted in Section 4 with a comparison to the distribu-

tion of satellite pericenter passage times in Section 4.1 and separately modeled as ram pressure stripping process in Section 4.2. We will discuss the implication of these results and conclude in Section 5.

## 2. OBSERVATIONS

Our goal in this work is to study satellite quenching as homogeneously as possible over a wide range of mass scales. This necessarily imposes constraints on our methods. In particular, in the absence of three-space velocities it is nearly impossible to select only satellite galaxies which are gravitationally bound to their hosts. We must instead rely on selecting any galaxies within some representative volume around a host as satellites, in this case all galaxies within 500 kpc of a host, keeping in mind that some fraction of these galaxies may be unbound or on first infall onto their host. All of our comparisons to simulations will be performed with the same selection process.

Covering a wide range of satellite masses requires us to combine observations from multiple sources. At the lowest masses we are limited to galaxies in the Local Group, which is itself a heterogeneous mixture of individually discovered dwarfs. To put some consistency in this data we use the compilation of McConnachie (2012), in which all known galaxies inside of 3 Mpc of the Sun are included. Each galaxy is classified with a ‘‘Morphological’’ Hubble type denoting it as either a star forming or a non-star forming type, though in general this classification is based on studies of resolved stellar populations rather than morphology alone. The presence of young stars and cold gas is usually sufficient to identify a Local Group galaxy’s star forming status, but in some cases there is either not sufficient data or a conflicting set of properties exist, making this determination difficult. These galaxies are marked as such (e.g., with a Hubble type ‘‘dIrr/dSph’’) in the McConnachie (2012) catalog, and in our figures we include this ambiguity of classification in the uncertainty on the quenched fraction. The other main quantity of interest for this work is the stellar mass of each galaxy, which is computed from the integrated absolute magnitude assuming a mass-to-light ratio of 1. This is inherently imprecise, but avoids the much more complex uncertainties present in dynamical measurements of the total mass of dwarf galaxies. The uncertainties in mass are relatively small compared to the wide mass bins we adopt, and thus a change in the overall mass to light ratio or even a systematic difference between star forming and quenched dwarfs only changes our reported quenched fractions by a factor smaller than the reported uncertainty from simply Poisson noise and classification difficulties.

Though the set of known Local Group satellites is certainly incomplete in an absolute sense, our focus on the relative fraction of star forming versus quenched galaxies minimizes the impact of this incompleteness. Over the volume and range of masses we consider here both dSphs and dIrrs are readily detected in the SDSS, as the red giant branch present in both can be detected out to at least 750 kpc (e.g., Slater et al. 2011; Bell et al. 2011). The bright stars present in dIrrs certainly make detection easier, but for any such dIrr that would fall in our sample a dSph of comparable mass and distance is also likely to be detectable. That is, over the area covered by the

SDSS the detection efficiency is high for both dSphs and dIrrs, and thus it is unlikely that our measured quenched fractions are strongly biased by differences in detectability. Furthermore, as our main result rests on the very high quenched fraction of low mass satellites, any bias in favor of detecting the brighter dIrrs would only reinforce this conclusion.

At the mid-range of masses, our sample comes from the NASA-Sloan Atlas of galaxies (NSA, Blanton et al. 2011). This sample reprocesses the images from the SDSS in a manner that better treats the extended surface brightness photometry required for large galaxies (on the sky) than the standard SDSS pipeline. The NSA also cross-matches sources with other large surveys and provides stellar masses estimated with the *kcorrect* software package (Blanton & Roweis 2007).

From this sample of galaxies, we wish to subselect only galaxies that are satellites of a more massive host. For this we closely follow the method used in Geha et al. (2012), which we summarize here. A sample of candidate ‘‘hosts’’ with  $M_{K_s} < -23$  (or approximately  $2.5 \times 10^{10} M_\odot$  in stellar mass) was compiled from SDSS and 2MASS and combined with several different sources of redshift data. This sample is designed to be complete out to  $z = 0.055$ , which is the redshift limit of the NSA. Each galaxy in the NSA was then matched with potential host galaxies by selecting the closest host galaxy on the sky with a difference in redshift less than  $1000 \text{ km s}^{-1}$ . The projected distance at the redshift of the host is then recorded as the physical separation.

In the work of Geha et al. (2012) this selection process was used to produce a very clean sample of isolated field dwarfs. In this work our purpose differs in that we require a clean sample of satellites with minimal numbers of projected ‘‘interlopers’’. This is a much more challenging selection process, since the significant peculiar velocities of satellites relative to their hosts requires a wide redshift cut, but such a cut also permits substantial numbers of isolated galaxies along the line of sight to be included as satellites. This is a fundamental limitation that cannot be easily remedied by changing the selection criteria, and instead we attempt to model and correct for the effect.

We can compute the number of interlopers that fall into our redshift cuts by constructing mock observations of an N-body simulation. We use the Millennium simulation for this purpose (Springel et al. 2005), which simulated a  $100 \text{ h}^{-1} \text{ Mpc}^3$  box. This is large enough that the observed volume of the NSA can fit within the simulation, simplifying the creation of the mock observations. From the simulation halo catalogs we create a catalog of ‘‘host’’ halos and a catalog of ‘‘dwarfs’’, differing only in their halo mass requirements. We apply the same redshift and projected separation cuts as for the observed data, then measure the fraction of these selected galaxies that actually lie within 500 kpc of their host. Since in the NSA our mass cuts are based on stellar masses, which are not directly available in the N-body simulation, we convert the stellar mass bins into halo mass bins using the relation from Moster et al. (2010), and also use this to set the limiting mass of a host halo.

The measured contamination fraction (interlopers over total number of selected galaxies) varies smoothly from

65% at the lowest stellar mass bin in the NSA to 51% at the highest mass bin. This relatively weak mass dependence limits the effects of uncertainties in the stellar mass determination, and testing with an artificially shallow relation (as could be caused by tidal stripping of satellites) does not substantially affect our results. The contamination fraction  $f_{\text{contam}}$  can directly be used to estimate the corrected quenched fraction  $f'_Q$ ,

$$f'_Q = f_Q + (f_Q - f_{FQ}) \left( \frac{f_{\text{contam}}}{1 - f_{\text{contam}}} \right), \quad (1)$$

where the inclusion of  $f_{FQ}$  for the fraction of quenched field galaxies accounts for the fact that some of the interlopers could themselves be quenched. Since this factor  $f_{FQ}$  is small, the effect of interlopers is to artificially lower the observed quenched fractions, while the high contamination fraction causes interlopers to constitute roughly half of the observed sample. The resulting correction is thus substantial, raising quenched fractions in the NSA from  $\sim 20\%$  to nearly 50% and underlining the importance of correcting these measurements. We note that interlopers primarily affect selection of satellite galaxies; the selection of field galaxies like in Geha et al. (2012) is much cleaner simply because the broad redshift cut only admits galaxies to the field sample if they are unambiguously isolated. There is unfortunately no such unambiguous criteria for satellites.

In addition to the contamination correction, it is also necessary to account for the relative volumes over which quenched and star-forming galaxies can be detected in the SDSS. To correct for this we weight each galaxy in the quenched fraction calculation by the inverse of the volume over which that galaxy could be detected, which is frequently referred to as a  $V_{\text{max}}$  correction<sup>1</sup>. This selection bias would otherwise drive the quenched fractions down, since the brighter star-forming galaxies would be over-represented. Using the  $V_{\text{max}}$  correction raises the final quenched fraction by 15-20%. We apply this correction only to the NSA sample, as it is impractical for the Local Group sample where an entirely heterogeneous set of surveys are responsible for the detection of dwarfs.

For the NSA sample we distinguish star-forming and quenched galaxies by a combination of the  $H\alpha$  equivalent width (EW) and the  $D_n4000$  measure of the break in the spectrum at  $4000\text{\AA}$ . We adopt the criteria of Geha et al. (2012), which required quenched galaxies to have an  $H\alpha$  EW less than  $2\text{\AA}$  and required  $D_n4000 > 0.6 + 0.1 \log_{10}(M_*/M_\odot)$ . The quenched fraction is not very sensitive to the specific value of the  $H\alpha$  cut; allowing galaxies with equivalent widths of  $4\text{\AA}$  to be counted as quenched only changes the resulting quenched fractions by 2-4%.

### 3. OBSERVATIONAL RESULTS

The resulting quenched fractions are shown as a function of satellite mass in Figure 1. There is some ambiguity inherent in the classifications of LG dwarfs into a binary “star-forming or quenched” system, so the error

<sup>1</sup> This  $V_{\text{max}}$  is not to be confused with the maximum circular velocity of a galaxy, which we will also use in the modeling section. Sorry.

bars on the LG quenched fraction extend from the lowest possible quenched fraction (assuming all ambiguous galaxies are star forming) to the highest possible fraction (assuming all ambiguous galaxies are quenched). While this is clearly not a statistical uncertainty, it does provide an illustration of the possible range of quenched fractions.

At the lowest-mass end, the data are consistent with nearly all satellites having no ongoing star formation. The lowest-mass satellite with evidence for recent star formation is Leo T, with a stellar mass of  $1.4 \times 10^5 M_\odot$  (under the M/L=1 assumption of McConnachie 2012), but determining the recent star formation history of such low mass galaxies is challenging (Weisz et al. 2012). Other examples of low-mass star forming dwarfs include LGS3 ( $9.6 \times 10^5 M_\odot$ ) and Phoenix ( $7.7 \times 10^5 M_\odot$ ), but these are substantially outnumbered by quenched dSphs at these masses. This is in spite of the fact that both types of galaxies down to masses of  $10^5 M_\odot$  (e.g., Draco) are well-detected to beyond the limits of the volume considered here, and that star forming dwarfs are generally easier to detect. Not until reaching masses of  $10^{6.5} - 10^8 M_\odot$  do substantial numbers of dIrrs begin to reduce the quenched fraction, with galaxies such as IC 10 ( $8.6 \times 10^7 M_\odot$ ), WLM ( $4.3 \times 10^7 M_\odot$ ) and IC 1613 ( $10^8 M_\odot$ ), for example. It’s worth noting that some of these galaxies may be on initial infall into the LG, and it could be argued that they are thus not representative of true satellites. While this could of course modify the absolute quenched fraction depending on the selection criteria, we argue that this does not affect the mass dependence we seek to illustrate. If there were no mass dependence in the quenched fraction, then where are the lower-mass star forming galaxies that are on first infall? Higher mass dwarfs are not preferentially infalling compared to lower mass dwarfs, as confirmed with the Via Lactea simulations, and we see little room for selection effects to cause the mass dependence we observe. The resulting conclusion is that some changing aspect of the quenching process itself must be responsible for this effect.

This drop-off in quenched fraction is corroborated by the NSA sample, which shows similar quenched fractions in the vicinity of 40-60%. This is an entirely independent measurement that shares very little in terms of potential observational biases with the LG data. We have not fine-tuned the quenching criteria in either sample to create this correspondence, as the criteria for both samples were originally defined by other works. The risk of detection biases related to the host-satellite distance are lessened in the NSA data, but they are replaced by projection and redshift-related effects. The principal uncertainty in the NSA measurement is the contamination correction, which changes the quenched fraction by roughly 20-30% in each bin. Even with such a substantial correction, the contamination fraction would have to be in the range of 80% or greater to bring the NSA quenched fractions as high as the seen in the LG.

Low quenched fractions at LMC-range masses are also seen in the work of Wheeler et al. (2014), which reached a similar conclusion with an alternate methodology. While we have corrected our observed sample for contamination by redshift-interlopers, Wheeler et al. (2014) has created mock observations of their models which include such

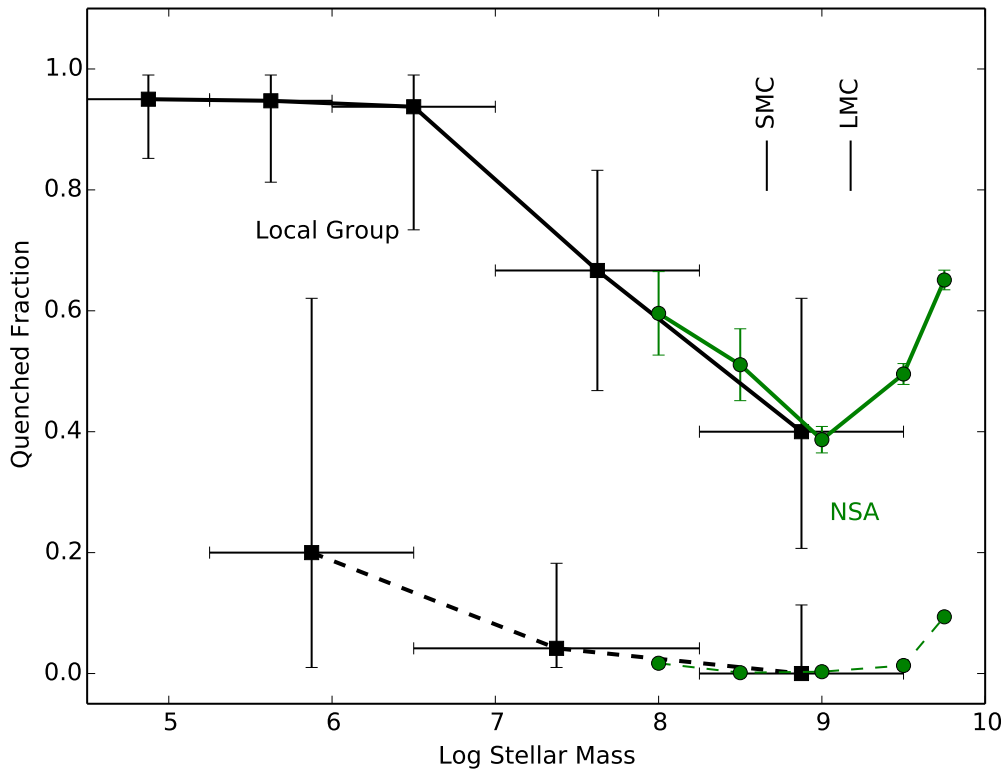


**Figure 1.** Fraction of quenched satellites as a function of galaxy stellar mass (solid line), along with fraction of quenched field galaxies (dashed line). The data comprise three samples: dwarfs in the Local Group (black squares), more massive satellites from the NSA catalog after correction for contamination (green circles). There is a clear transition near  $10^7 - 10^8 M_{\odot}$  from nearly ubiquitous quenching of satellites at low mass to much lower quenched fractions at higher masses.

contamination and left the observations unchanged. Either process should be equally valid, and the similarity in resulting values provides an additional confirmation of our conclusions, but the difference between methods should be noted in making any direct comparisons. In particular our correction for contamination is necessary to homogenize the NSA quenched fractions with observations of the Local Group, which do not suffer from this problem. We also note that the host galaxies of the NSA satellites are not selected to have a common mass. This may have implications if the relative mass of satellite and host is an important determinant of quenching, but in general we expect that the inclusion of LMC-mass galaxies around much larger hosts than the Milky Way would serve to raise the quenched fraction rather than lower it, thus minimizing the difference between the mass ranges rather than artificially increasing the difference. The conclusion of a substantially lower quenched fraction from  $10^{7.5}$  to  $10^{9.5} M_{\odot}$  appears robust.

In addition to the fraction of quenched satellites, we also show the fraction of quenched field galaxies from both the NSA and the Local Group. As shown by Geha et al. (2012), quenched field galaxies are extremely uncommon at stellar masses below  $10^9 M_{\odot}$ . The causes of this behavior are beyond the scope of this work, but we show this to demonstrate that the quenched fraction of satellites at the masses we are interested in is set primarily by interactions, and not set by quenching of galaxies

in the field. This is certainly true in the NSA sample, where there is less room for observational biases to act differentially on field and satellite populations.

We note that the sample of field galaxies at stellar masses of  $10^7 M_{\odot}$  may be incomplete, since such intrinsically faint galaxies at distances of 1 Mpc and greater are observationally challenging. This also affects field dSphs more than field dIrrs due to their differences in intrinsic luminosity at fixed stellar mass. For these reasons we do not want to make any firm statements about the lack of field dSphs. In the LG sample we know of only a single field galaxy, KKR 25 (Makarov et al. 2012), that appears quenched, but it would be difficult to extrapolate from this one galaxy whether a larger population of field dSphs exists or if this galaxy is somehow peculiar. In our modeling we will assume that no dwarfs are quenched in the field, but we acknowledge that this is not yet certain and could be open to revision.

#### 4. QUENCHING MODELS

Given the changes in the quenched fraction that we see, we would like to understand how this population-based observation can constrain physical models for the quenching process. To restate it simply, if we seek to create a scenario in which 50% of the high mass dwarfs are quenched, we need to find a criterion for quenching which is met by only 50% of the dwarfs at that mass. In this work we posit two such possible criteria: one which is

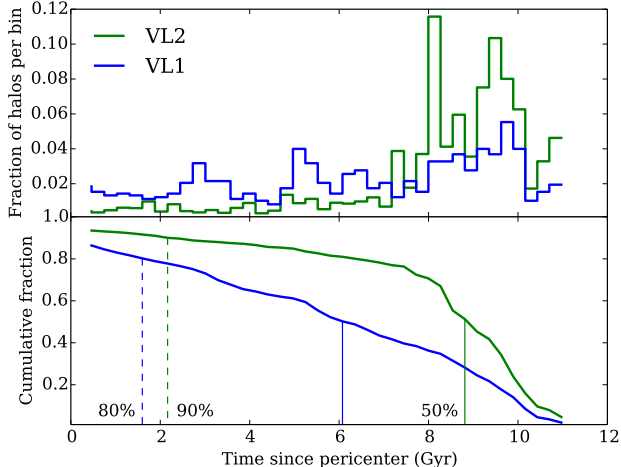


**Figure 2.** Differential (top panel) and cumulative distribution (bottom panel) of time between a satellite’s first pericenter passage and  $z = 0$ , shown for both Via Lactea simulations. The solid vertical lines indicate where the cumulative distribution exceeds 50%, while the dashed vertical lines indicate 80% and 90%. This provides a direct estimate of the quenching delay time that would be required to produce a desired quenched fraction. To reproduce the quenched fraction of the highest mass LG dwarfs thus requires a delay of 6-9 Gyr between pericenter passage and quenching, under this model. To reproduce a quenched fraction of 80% or more for low mass galaxies, noting that 10-15% of selected halos have not yet experienced a pericenter passage, short quenching times of order 2 Gyr are required.

based on the time since a galaxy’s first pericenter passage around its host, and another based on the maximum ram pressure experienced by each dwarf. We can then set the parameters of these criteria such that they reproduce the observed mass dependence of quenched fraction.

This goal of these models is to illustrate the magnitude of the change in the quenching criteria with mass required to match the observations, and to put physical constraints on possible quenching mechanisms based on our observations of the populations. We note that these simplified models are each taken in isolation, requiring the change in quenching fraction to be the result of a single parameter, when in reality there may be several factors that all combine to produce the observed population. While detailed hydrodynamical simulations are required for any *ab initio* modeling of the quenching process, these simple models will hopefully demonstrate the magnitude of the problem.

#### 4.1. Quenching Delay Time

We first seek to model the changing quenched fraction by positing that the time since the satellite’s first pericenter passage around the host is the critical parameter. This “delay time” model may be interpreted differently depending on the physical mechanism involved; for example, for large galaxies falling into clusters the delay time could correspond to a scenario where gas accretion onto the satellite is stopped upon infall, but some additional time is required for the star formation to consume the pre-existing gas. This is primarily of interest when the delay time, as measured in population studies, is roughly the same duration as the gas consumption timescale for a galaxy. Such a delay time has been used to model the

quenching of massive galaxies by Wetzel et al. (2013), but we note that our model differs in that we assume instantaneous quenching after a delay, whereas Wetzel et al. (2013) have both a delay and a timescale for star formation to decay. Since we lack both specific star-formation rates for the dwarfs and sufficient numbers of dwarfs to disentangle these effects, the assumption of instantaneous quenching will suffice.

The cumulative distribution of satellite infall times is shown in Figure 2, with the original Via Lactea run in blue and Via Lactea II shown in green to illustrate the scatter between halo realizations. From this figure we can see the delay time that would be required for a given fraction of satellites to remain star-forming in this model. The solid vertical lines are drawn where the cumulative fraction of satellites that have undergone pericenter is 0.5, which is roughly the quenched fraction observed for satellites at  $10^8 - 10^{10} M_{\odot}$ . The dashed vertical lines are drawn at cumulative fractions of 80% and 90%, which is characteristic of the low mass quenched fractions observed in the Local Group.

These cumulative pericenter fractions suggest that a rapid quenching process with a median delay time of  $\sim 2$  Gyr is sufficient to reproduce the high fraction of quenched satellites seen in the LG, though considerable scatter exists between simulations. This rapid quenching is required to maintain the high quenched fraction, as recently-infalling satellites would tend to depress the quenched fraction if they were not quenched quickly. Rapid quenching upon pericenter also dovetails well with the observed radial distribution of dSphs. In a previous work (Slater & Bell 2013) we showed that reproducing the radial distribution of quenched LG dwarfs via a close interaction with the host requires a single such pericenter passage to be sufficient for quenching; any scenario in which more than one pericenter is required is strongly excluded by the existence of quenched dwarfs at  $\sim 700$  kpc. Rapid removal of gas on a single pericenter fits both the high quenched fraction and the radial dependence quite well in the LG.

This short quenching time stands in contrast to the very long gas consumption timescales of these dwarfs. In general, dIrrs in the field frequently have as much cold gas as they have stars, if not more (Grcevich & Putman 2009), and at their mean star formation rates many are unlikely to consume their gas in less than a Hubble time (Hunter & Gallagher 1985; Bothwell et al. 2009; Huang et al. 2012). The short timescale for quenching that we measure reaffirms that the cut-off of gas accretion cannot be responsible for quenching low mass satellites; such a mechanism would leave far too many star forming dwarfs in the LG to match the observations. A rapid *removal* of cold gas appears to be necessary to quench a sufficient number of low mass satellites in a short period of time.

In comparison to the rapid quenching times for low mass dwarfs, Figure 2 suggests that to reproduce the roughly 50% quenched fraction at the masses characteristic of the NSA, a median delay time of 6-9 Gyr is required. This is in line with the conclusions of Wheeler et al. (2014) that satellite quenching at these masses is inefficient. Though this observation is clear, the cause of such inefficiency is difficult to determine since it can be the result of a quenching process which is either slow or which operates only on select dwarfs. It is possible that

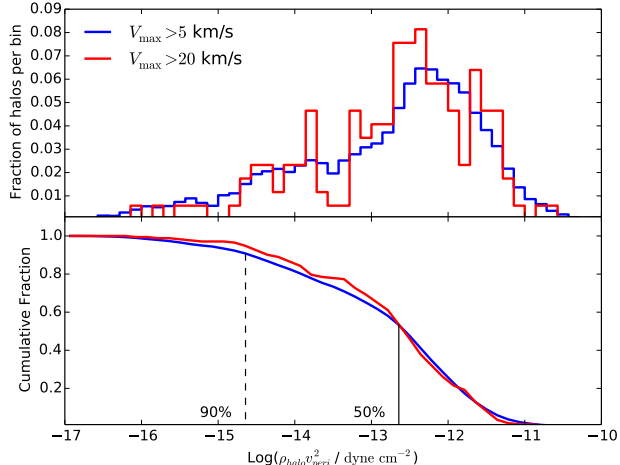


**Figure 3.** Histogram of the maximum ram pressure experienced by halos in the Via Lactea simulation (top), along with the cumulative distribution of ram pressures (bottom). The data are split into all halos with  $V_{\max} > 5$  km/s in blue, and only halos with  $V_{\max} > 20$  km/s in red, to show that the ram pressure distribution is largely independent of satellite mass. From the cumulative plot we can read the ram pressure required for quenching either 90% or 50% of satellites, and note that the two values differ by roughly a factor of 100.

the time since pericenter is truly a clock which quenches galaxies that have been satellites for 6-7 Gyr or greater, and that all unquenched satellites are more recent additions to the LG. This scenario could arise if infall stopped the accretion of gas and the delay before a galaxy became quenched was set by the gas consumption time. However, this is not the only possible interpretation. For example, Wheeler et al. (2014) suggests that using the degree of mass loss as a proxy for the strength of interactions with the host is a more reasonable parameterization for what stops a dwarf’s star formation. While it is possible that time since pericenter is not the factor that *determines* if a galaxy is quenched, it is unavoidable that some LMC-mass galaxies have been forming stars as satellites for as much as 6-7 Gyr after their first pericenter passage. If there were not, and only recent accretions could continue to form stars, the quenched fraction would necessarily be much higher at these masses. Thus while the evidence is inconclusive as to whether time is the dominant factor in quenching, whatever does cause quenching at these masses must permit some satellites to continue to form stars for many gigayears.

#### 4.2. Ram Pressure

A possible mechanism for the removal of gas from satellites is ram pressure stripping by hot gas surrounding galaxies and clusters. Initially suggested to explain the relative infrequency of spiral galaxies in clusters (Gunn & Gott 1972), the presence of hot halos around galaxies has been suggested as a way of accounting for the deficit of baryons present in the stars and cold gas of galaxies when compared to the cosmological baryon fraction (Fukugita et al. 1998; Read & Trentham 2005; Cen & Ostriker 1999). Though the observed halos may not be massive enough to contain all of the missing baryons (Benson et al. 2000; Anderson & Bregman 2010), they may still be able to affect the satellites passing through

the hot gas (Lin & Faber 1983; Mayer et al. 2006; McConnachie et al. 2007).

As noted above, the short timescales required for quenching at low masses appears to fit naturally with a model where the bulk of the satellite’s cold gas is removed quickly by ram pressure stripping. The ram pressure force experienced by a galaxy is  $\rho v^2$ , where  $\rho$  is the density of the gas the satellite moves through and  $v$  is its velocity. These two factors are greatest when a galaxy passes pericenter around its host, thus causing an “impulsive” effect on the satellite. The response of a satellite to such a force will clearly depend on its mass distribution, which determines how strongly it can hold on to its cold gas. However, the mass distribution of gas, stars, and dark matter in dIrrs is uncertain, and the magnitude of the restoring force which resists stripping is difficult to compute *a priori* for dwarfs of differing masses. Our modeling seeks to circumvent this problem by measuring ram pressure experienced by the population of satellites, and then use this to constrain how individual galaxies must respond. Other studies in the LG (e.g., Grcevich & Putman 2009; Gatto et al. 2013) have sought to use the distribution of stripped and non-stripped dwarfs to constrain the density profile of the Milky Way’s hot halo. We wish to turn this around; using a model of the halo from X-ray absorption studies (Miller & Bregman 2013), what would the quenching criterion have to be to reproduce the observed quenched fractions?

To compute this, we want to estimate the range of pressures experienced by satellites as they fall into their host. At each of these pericenters we can compute the hot gas density, which together with the orbital velocity gives us the ram pressure force  $\rho v^2$ . To obtain the kinematic information on satellite halos we use both the Via Lactea and the Via Lactea II simulations (Diemand et al. 2007, 2008), which sought to reproduce a Milky Way-like environment in a dark-matter-only simulation and together provide a rough estimate of the scatter between halo realizations. Using these N-body simulations lets us avoid the uncertainties of hydrodynamic simulations of ram pressure stripping, in which small satellites are difficult to resolve given the enormous dynamical range required. We track the orbit of each surviving subhalo in the simulations through each of its pericenter passages around either the Milky Way-mass halo or “Halo 2”, a rough analog of the Andromeda that appears in VL2 (see Slater & Bell 2013; Teyssier et al. 2012, for further details on Halo 2). In finding the pericenter distances of subhalos we interpolate between snapshots in the simulation, which prevents pericenter distances from being overestimated due to the limited number of snapshots. As we showed in Slater & Bell (2013), we have used the more frequent snapshots in the VL1 simulation to verify that interpolation does not add significant errors.

In this model we assume that the single closest pericenter passage is entirely responsible for stripping. This is motivated by the strong velocity dependence of ram pressure, in which pericenter passages should dominate over the rest of the galaxy’s orbit, but also imposed by uncertainties in the cumulative effect of ram pressure over an extended period of time or multiple pericenter passages.

From the closest pericenter we compute the density of the host galaxy’s hot halo, using the Miller & Bregman (2013) model of the Milky Way as an example density

profile. Their work uses a  $\beta$ -model for the functional form of the profile, constrained by measurements of X-ray absorption against various extragalactic and galactic sources, with a total hot gas mass of  $3.8 \times 10^{10} M_{\odot}$  inside of 200 kpc. We note that this is a measurement of the present-day halo, and the halo may have been weaker or non-existent in the past. In assigning gas pressures seen by halos in the past we should be using the halo profile present at that time, but the evolution of hot gas halos is even more uncertain than the structure of halos that exist today. We thus make as simple of an assumption as is plausible, that the halo has had the same structure and mass since  $z = 1$ , before which it did not exist. This cut-off redshift is not critical to the results, and could even be omitted entirely without significant changes, as the majority of satellites have short enough orbital periods that they have a pericenter passage after the halo has turned on. If the density of the hot halo were to change substantially at very late times then it may have a more significant effect on our results, but any such halo growth would be entirely an assumption.

The resulting distribution of peak  $\rho v^2$  values seen by the subhalos in Via Lactea is shown in Figure 3. The top panel shows a histogram of these values, while the bottom panel shows the cumulative distribution. In both panels the blue line samples all halos in the simulation with a maximum circular velocity at  $z = 0$  of  $V_{\max} \geq 5$  km/s, while the red line only includes halos with  $V_{\max} \geq 20$  km/s. While this division is arbitrary, we include it to show that there is no significant correlation between satellite masses and the ram pressures they experience, so we will treat the results we derive from orbits as essentially independent of mass.

This bottom panel can be read as the fraction of galaxies that have experienced ram pressure of *at least* a given strength; in case we see that 90% of all halos have seen ram pressure in excess of  $10^{-14.8}$  dyne  $\text{cm}^{-2}$ , while only 50% have experienced pressures greater than  $10^{-12.8}$  dyne  $\text{cm}^{-2}$ . This is the key result of this model. If we ascribe the entirety of the quenched fraction change between  $M_{\star} = 10^6$  and  $10^{7.5} M_{\odot}$  to changes in a galaxy's response to a given force of ram pressure, then it is this factor of 100 change in pressure that galaxy models must account for.

Such a model would need to treat the changing gas densities, stellar disk densities, and dark matter halo all to obtain a better estimate of the quenching criterion. This can be seen schematically by rewriting the force balance from Gunn & Gott (1972) in terms of surface densities (Mo et al. 2010),

$$\rho v^2 \sim 2\pi G \Sigma_{\star} \Sigma_{\text{gas}}, \quad (2)$$

where now the relative distribution of stars and gas may lead to both a complicated dependence on total mass and could also suggest varying degrees of partial stripping in some cases. Unfortunately these mass distributions are not well constrained observationally, and the dark matter distribution may also play a role if its contribution to the restoring force is more significant than the stellar density (Abadi et al. 1999). This is difficult to assess from an observational standpoint, as the behavior of gas which is hypothetically stripped from the disk but remains bound to the dwarf is unclear. Even so, better

models of dIrrs may not produce more accurate results if the underlying assumption of a stripping criterion based on force balance is itself inaccurate. This has been suggested by simulations that better treat the hydrodynamic instabilities in interactions, resulting in a stripping that proceeds more via ablation than by impulsive momentum transfer (Weinberg 2013). Similarly, the addition of tidal effects during pericenter passage (Mayer et al. 2006) or internal heating by star formation (Nichols & Bland-Hawthorn 2011) could play a significant role in determining a satellite's response to ram pressure and particularly the dependence on satellite mass. The sum of these uncertainties both in models of dIrrs and in the physics of stripping limit our ability to provide a more detailed explanation for the evolution in stripping efficiency, but the magnitude of the effect is clearly demonstrated in the range of ram pressure forces experienced.

## 5. DISCUSSION AND CONCLUSIONS

We have shown that the fraction of quenched satellite galaxies undergoes significant variation across masses ranging from low mass dwarfs around the Milky Way and Andromeda to more massive satellites in the LG and beyond. This a measurement spanning five orders of magnitude in mass, which highlights the commonality of satellite quenching as a phenomenon but conversely the large span of masses should also temper our surprise that a complex process like quenching exhibits varied behavior at different masses. The structure of galaxies across this range of masses changes substantially, and hence their strongly differing response to environmental factors may be a reflection of that fact.

We argue that our conclusion of a rapid quenching process for low mass satellites is unavoidable given the ubiquity of quenched satellites at these masses. The speed of quenching immediately places a constraint on plausible mechanisms, and the rapid removal of gas by ram pressure stripping appears to be a logical possibility. Quenching processes that proceed on the gas consumption timescale are difficult to reconcile with the observations. At the masses of the NSA sample, where the quenched fraction is closer to 50% than 90%, the long delay times leave the question of physical mechanisms open. Here the issue of a time delay may interact with repeated pericenter passages to remove gas only gradually in these massive dwarfs. Such a scenario is both beyond the capabilities of our model and poorly understood physically.

Our model of ram pressure stripping has sought to illustrate how dwarfs of differing masses must respond to ram pressure, if it is the dominant source of quenching. This method turns the observed quenched fractions into a value for the cut-off ram pressure between stripping and leaving a galaxy to continue forming stars, which provides a characterization of the forces at work. As with the delay time, it is possible that additional factors add complications to our picture of a simple ram pressure cut-off. For instance, the inclination of the disk of a dIrr as it falls into the galaxy may tip the balance if it would otherwise be on the cusp of being stripped. We argue that our characterization of the factor of 100 change in ram pressure seen by 50% and 90% of satellites provides an estimate of the average behavior, which may not apply to each satellite individually.

While our modeling has attempted to assess the general characteristics of satellite quenching, our models are clearly not the *ab initio* models of quenching that could explain the mechanisms behind the observed behavior. We emphasize the importance of attempts to construct such models in order to narrow what is presently a wide-open range of physical processes that are suggested to affect quenching. Accurate modeling of the input dIrr galaxies to be stripped is also critical in this effort, since our understanding of the stripping process requires detailed knowledge of the systems to be stripped. We have shown at a basic level what evolution in this effectiveness one might expect with mass, but this does not attempt to account for the changes in dwarf structure with mass. What was set up in Gunn & Gott (1972) as a simple force balance between ram pressure and the restoring force likely has substantial uncertainties on both sides.

We also must emphasize an important caveat of our study, which is that all of our data below  $M_* = 10^{7.5} M_\odot$  comes from satellites of the Milky Way and Andromeda. While we argue that these data are robust, the limited number of systems makes it impossible to know if the high quenched fractions are truly universal across Milky Way-like systems, or whether they are a peculiar result tied to the specific accretion history of the Local Group. This is a particularly important question in the light of results suggesting that the quenched fraction of satellites is dependent on whether or not the central galaxy is forming stars, an observation referred to as “galactic conformity” (Weinmann & Lilly 2005; Phillips et al. 2014). We note that our Local Group results show a high fraction of quenched satellites around what are clearly star-forming hosts (the Milky Way and Andromeda). This perhaps illustrates the lower limit at which galactic conformity is effective; the lowest mass dwarfs appear to quench regardless of their host.

Despite this potential complication at LMC-masses, in the absence of any further information our best estimate of the quenching behavior comes from assuming that our galaxy is “average” and does truly represent a universal behavior, but we would surely have greater confidence if observations of other systems could confirm this universality rather than leave it as an assumption. This is but one of many subjects that stand to gain from the development of larger samples of dwarfs beyond the Local Group.

This work was supported by NSF grant AST 1008342. We again thank the Via Lactea collaboration for making their simulation outputs publicly available, and M. Geha for both productive discussions and for providing the host galaxy catalog.

#### REFERENCES

Abadi, M. G., Moore, B., & Bower, R. G. 1999, MNRAS, 308, 947  
Anderson, M. E., & Bregman, J. N. 2010, ApJ, 714, 320

- Balogh, M. L., Baldry, I. K., Nichol, R., et al. 2004, ApJ, 615, L101  
Bell, E. F., Slater, C. T., & Martin, N. F. 2011, ApJ, 742, L15  
Benson, A. J., Bower, R. G., Frenk, C. S., & White, S. D. M. 2000, MNRAS, 314, 557  
Blanton, M. R., & Roweis, S. 2007, AJ, 133, 734  
Blanton, M. R., Kazin, E., Muna, D., Weaver, B. A., & Price-Whelan, A. 2011, AJ, 142, 31  
Bothwell, M. S., Kennicutt, R. C., & Lee, J. C. 2009, MNRAS, 400, 154  
Cen, R., & Ostriker, J. P. 1999, ApJ, 514, 1  
Cole, S., Aragon-Salamanca, A., Frenk, C. S., Navarro, J. F., & Zepf, S. E. 1994, MNRAS, 271, 781  
Chiboucas, K., Jacobs, B. A., Tully, R. B., & Karachentsev, I. D. 2013, arXiv:1309.4130  
Dekel, A., & Silk, J. 1986, ApJ, 303, 39  
Dijkstra, M., Haiman, Z., Rees, M. J., & Weinberg, D. H. 2004, ApJ, 601, 666  
Diemand, J., Kuhlen, M., & Madau, P. 2007, ApJ, 667, 859  
Diemand, J., Kuhlen, M., Madau, P., et al. 2008, Nature, 454, 735  
Dressler, A. 1980, ApJ, 236, 351  
Efstathiou, G. 1992, MNRAS, 256, 43P  
Ferrara, A., & Tolstoy, E. 2000, MNRAS, 313, 291  
Font, A. S., Bower, R. G., McCarthy, I. G., et al. 2008, MNRAS, 389, 1619  
Fukugita, M., Hogan, C. J., & Peebles, P. J. E. 1998, ApJ, 503, 518  
Geha, M., Blanton, M. R., Yan, R., & Tinker, J. L. 2012, ApJ, 757, 85  
Gunn, J. E., & Gott, J. R., III 1972, ApJ, 176, 1  
Gatto, A., Fraternali, F., Read, J. I., et al. 2013, MNRAS, 433, 2749  
Grevech, J., & Putman, M. E. 2009, ApJ, 696, 385  
Gnedin, N. Y. 2000, ApJ, 542, 535  
Huang, S., Haynes, M. P., Giovanelli, R., et al. 2012, AJ, 143, 133  
Hunter, D. A., & Gallagher, J. S., III 1985, ApJS, 58, 533  
Lin, D. N. C., & Faber, S. M. 1983, ApJ, 266, L21  
Makarov, D., Makarova, L., Sharina, M., et al. 2012, MNRAS, 425, 709  
Mayer, L., Mastropietro, C., Wadsley, J., Stadel, J., & Moore, B. 2006, MNRAS, 369, 1021  
McConnachie, A. W., Venn, K. A., Irwin, M. J., Young, L. M., & Gehan, J. J. 2007, ApJ, 671, L33  
McConnachie, A. W. 2012, AJ, 144, 4  
Miller, M. J., & Bregman, J. N. 2013, ApJ, 770, 118  
Mo, H., van den Bosch, F. C., & White, S. 2010, Galaxy Formation and Evolution, by Houjun Mo, Frank van den Bosch, Simon White, Cambridge, UK: Cambridge University Press, 2010,  
Moster, B. P., Somerville, R. S., Maulbetsch, C., et al. 2010, ApJ, 710, 903  
Nichols, M., & Bland-Hawthorn, J. 2011, ApJ, 732, 17  
Phillips, J. I., Wheeler, C., Boylan-Kolchin, M., et al. 2014, MNRAS, 437, 1930  
Postman, M., & Geller, M. J. 1984, ApJ, 281, 95  
Read, J. I., & Trentham, N. 2005, Royal Society of London Philosophical Transactions Series A, 363, 2693  
Sawala, T., Scannapieco, C., Maio, U., & White, S. 2010, MNRAS, 402, 1599  
Slater, C. T., Bell, E. F., & Martin, N. F. 2011, ApJ, 742, L14  
Slater, C. T., & Bell, E. F. 2013, ApJ, 773, 17  
Springel, V., White, S. D. M., Jenkins, A., et al. 2005, Nature, 435, 629  
Teyssier, M., Johnston, K. V., & Kuhlen, M. 2012, MNRAS, 426, 1808  
Tinker, J. L., & Wetzel, A. R. 2010, ApJ, 719, 88  
van den Bosch, F. C., Aquino, D., Yang, X., et al. 2008, MNRAS, 387, 79  
Weinberg, M. D. 2013, arXiv:1304.3942  
Weinmann, S. M., & Lilly, S. J. 2005, ApJ, 624, 526  
Weinmann, S. M., van den Bosch, F. C., Yang, X., & Mo, H. J. 2006, MNRAS, 366, 2  
Weinmann, S. M., Kauffmann, G., von der Linden, A., & De Lucia, G. 2010, MNRAS, 406, 2249  
Weisz, D. R., Zucker, D. B., Dolphin, A. E., et al. 2012, ApJ, 748, 88  
Wetzel, A. R., Tinker, J. L., Conroy, C., & van den Bosch, F. C. 2013, MNRAS, 432, 336  
Wheeler, C., Phillips, J. I., Cooper, M. C., Boylan-Kolchin, M., & Bullock, J. S. 2014, MNRAS, 442, 1396